Chemistry–A European Journal
Research Article
doi.org/10.1002/chem.202400935
Chemistry Europe
European Chemical Societies Publishing
www.chemeurj.org

Hot Paper

Low-lying LUMO Boosts Conductance in Antiaromatic Dibenzopentalene Versus Aromatic Analogues

Maximilian Schmidt,[a] Lydia Abellán Vicente,[b] M. Teresa González,[b] Linda A. Zotti,*[c, d] Birgit Esser,*[a] and Edmund Leary*[b]

Dedicated to Professor Miquel Solà on the occasion of his 60th birthday

Antiaromaticity is a fundamental concept in chemistry, but the study of molecular wires incorporating antiaromatic units is limited. Despite initial predictions, very few studies show that antiaromaticity has a beneficial effect on electron transport. Dibenzo[*a*,*e*]pentalene (DBP) is a stable structure that displays appreciable antiaromaticity within the five-membered rings of the pentalene core. We have investigated derivatives of DBP furnished with pyridyl (Py) and F_4-pyridyl (PyF_4) anchor groups, and compared the conductance with purely aromatic phenyl and anthracene analogues. We find that the low-bias conductance of **DBP-Py** is approximately 60% larger than that of the anthracene analogue **Anth-Py** and 250% larger compared to the phenyl derivative **Ph-Py**. This is due to a better alignment of the LUMO with the gold Fermi level, which we confirm by conductance-voltage spectroscopy where the conductance of **DBP-Py** shows the greatest voltage-dependence. The F_4-pyridyl compounds, which have lower LUMO energies compared to the pyridyl analogues, did not, however, form detectable molecular junctions. The strongly electron-withdrawing fluorine atoms reduce the donor capability of the nitrogen lone-pair to the point where stable N–Au bonds no longer form.

Introduction

One of the principle aims of molecular electronics is to relate electron transport behaviour to chemical properties of molecules, such as the degree of conjugation or the size of the HOMO–LUMO gap. In this regard, different structure-property studies have been performed, with many showing how transport across molecular junctions depends strongly on the molecular backbone. One clear example is the effect of quantum interference (QI) on molecular conductance.[1,2] Due to the wave-nature of the transmitted electrons, conductance is either enhanced or suppressed depending on the frontier molecular orbital symmetries.[3] This can be quite precisely controlled through manipulation of just single sites along the backbone or the positioning of the anchor groups.[4–7] Moreover, also the nature of the anchor groups, the electrode material as well as the environment have all been shown to play a significant role.[8] For instance, the type of anchoring group is known to affect the electrical conductance by modifying the energy alignment of the frontier orbitals.[9,10]

Many molecular wires explored to date contain aromatic and heteroaromatic rings, and some systematic studies have linked the degree of aromaticity to the magnitude of the low-bias conductance. In one of the first studies, Chen *et al.*, observed that for a family of amine-terminated compounds, the thiophene derivative had the lowest conductance, the furan was slightly higher and the cyclopentadiene the highest.[11] As thiophene is more aromatic than furan, and cyclopentadiene is non-aromatic, the conductance is, thus, anticorrelated with aromaticity. This behaviour was also found for a series of compounds with tricyclic cores, although with some specific exceptions.[12] Theoretical work by Borges *et al.* supports the idea that aromaticity inhibits transport.[13] Rather importantly, however, there are also systematic studies which have failed to find any correlation between conductance and aromaticity, such as the studies by Yang *et al.* and Miguel *et al.* into 5- and 6-membered heterocyclic compounds, respectively.[14,15]

[a] *M. Schmidt, Prof. Dr. B. Esser*
Institute of Organic Chemistry II and Advanced Materials
Ulm University
Albert-Einstein-Allee 11, 89081 Ulm, Germany
E-mail: birgit.esser@uni-ulm.de
Homepage: www.esserlab.com

[b] *L. Abellán Vicente, Dr. M. T. González, Dr. E. Leary*
Fundación IMDEA Nanociencia
Calle Faraday 9
Campus Universitario de Cantoblanco, 28049 Madrid, Spain
E-mail: edmund.leary@imdea.org

[c] *Dr. L. A. Zotti*
Departamento de Física Teórica de la Materia Condensada
Universidad Autónoma de Madrid
28049, Madrid, Spain
E-mail: linda.zotti@uam.es

[d] *Dr. L. A. Zotti*
Institute of Condensed Matter Physics (IFIMAC)
Universidad Autónoma de Madrid
28049, Madrid, Spain

Supporting information for this article is available on the WWW under https://doi.org/10.1002/chem.202400935

With this slightly confused picture in mind, it makes sense to explore molecular wires that contain 4n π-electron rings, formally making them Hückel antiaromatic, and to compare them to 4n + 2 aromatic analogues. One might expect the behaviour of antiaromatic compounds to oppose that of aromatic compounds, such that those displaying a higher degree of antiaromaticity should generally have higher conductances. This was indeed found by Fujii *et al.* who compared a 16 π-electron nickel norcorrole (NiNc-SAc) with its 18 π-electron porphyrin (NiP-SAc) analogue.[16] The former displayed a conductance approximately 20 times greater than the latter, which was attributed to the antiaromaticity of norcorrole. Some of this difference may be attributed to the slightly shorter molecular length as to norcorrole has two fewer carbons within its ring. In the junction, the rings of NiNc-SAc and NiP-SAc may also adopt slightly different conformations, such as planar, domed or ruffled geometries,[17] that could also slightly affect the conductance. The overall conclusion, however, is that the antiaromaticity of NiNc-SAc dominates, leading to the increased conductance. Conversely, Gantenbein *et al.* studied a series of biphenylene derivatives, which contained a (much smaller) 4 π-electron ring at the centre.[18] Compared to aromatic analogues containing naphthalene, anthracene and fluorene units, the biphenylene compounds were, in fact, slightly less conductive. The authors concluded that the partially antiaromatic bonding at the centre was too weak an effect to have a visible influence on the charge transport.

We previously studied a DBP derivative using thioanisole anchor groups with the molecular break-junction (BJ) technique and compared its conductance with phenyl and anthracene variants (**DBP-SMe**, **Ph-SMe** and **Anth-SMe**, respectively).[19] Both **DBP-SMe** and **Anth-SMe** had a higher conductance than **Ph-SMe**, but the difference between the DBP and anthracene compounds was close to the limits of resolution of the technique. Theoretical simulations showed that the energetic alignment of the frontier molecular orbital with respect to the Fermi level controls the conductance ratio.[19] Despite **DBP-SMe** having the smallest HOMO–LUMO energy gap, unfavourable energy level alignment in the junction resulted in a similar conductance at the Fermi level compared to the anthracene derivative. We hypothesised that if we could direct the compounds to conduct predominantly via their unoccupied states, a greater difference would be seen between DBP and phenyl/anthracene. This is based on the fact that for **DBP-SMe**, the LUMO is strongly coupled to the electrodes, and was significantly lower in energy than the LUMOs of **Ph-SMe** and **Anth-SMe**. We have previously shown that the DBP core typically yields compounds with low-lying LUMO energy levels.[20]

In this study, our goal was to direct transport through the unoccupied levels and to assess the resulting dependence of the conductance on the nature of the central group (aromatic versus antiaromatic). To this end, we designed a family of molecular wires containing phenyl (Ph) and anthracene (Anth) (both aromatic) and dibenzo[*a*,*e*]pentalene (DBP, antiaromatic) cores, and terminated them with pyridyl anchor groups (**Ph-Py**, **Anth-Py** and **DBP-Py**, respectively (upper panel, Figure 1).

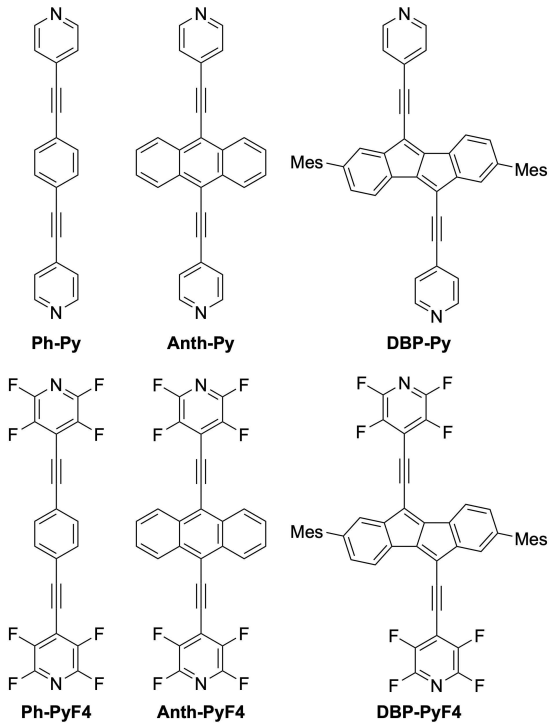

Figure 1. Structures of compounds under investigation in this study.

Pyridyls have been shown to give rise to LUMO-dominated transport both theoretically and experimentally via the sign of the measured Seebeck coefficients.[21,22] In order to lower the LUMO levels further, we also investigated the fluorinated analogues **Ph-PyF$_4$**, **Anth-PyF$_4$** and **DBP-PyF$_4$** (lower panel, Figure 1).

Results and Discussion

Synthesis of Pyridyl and F$_4$-Pyridyl Derivatives

The DBP derivatives were synthesized in a similar manner as described before (Scheme 1, full details are shown in SI).[19,20] Mesityl substituents were chosen to enhance solubility of the DBP derivatives. Diol **1** was coupled in a Sonogashira-reaction with the respective iodo- or bromopyridine derivative to furnish **2a** and **2b**. Due to the strongly electron-withdrawing character of the pyridines, water elimination using *p*TsOH was not successful, and trifluoroacetic anhydride at elevated temperature had to be used to obtain **DBP-Py** and **DBP-PyF$_4$** in moderate yields of 41% and 26%, respectively, over two steps.

The aromatic analogues **Ph-Py** and **Anth-Py** were obtained in good yields of 75% and 73% from the bis((trimethylsilyl)ethynyl) derivatives **3** and **4**, respectively, by deprotection of the alkynes using K_2CO_3 followed by Sonogashira-reaction with 4-iodo-pyridine. For the poorly soluble fluorinated compounds purification was unsuccessful. Here, another strategy developed by Alabugin *et al.* was used, which involved an *in situ* deprotection of the TMS-groups and direct nucleophilic attack of the formed acetylide on pentafluoropyr-

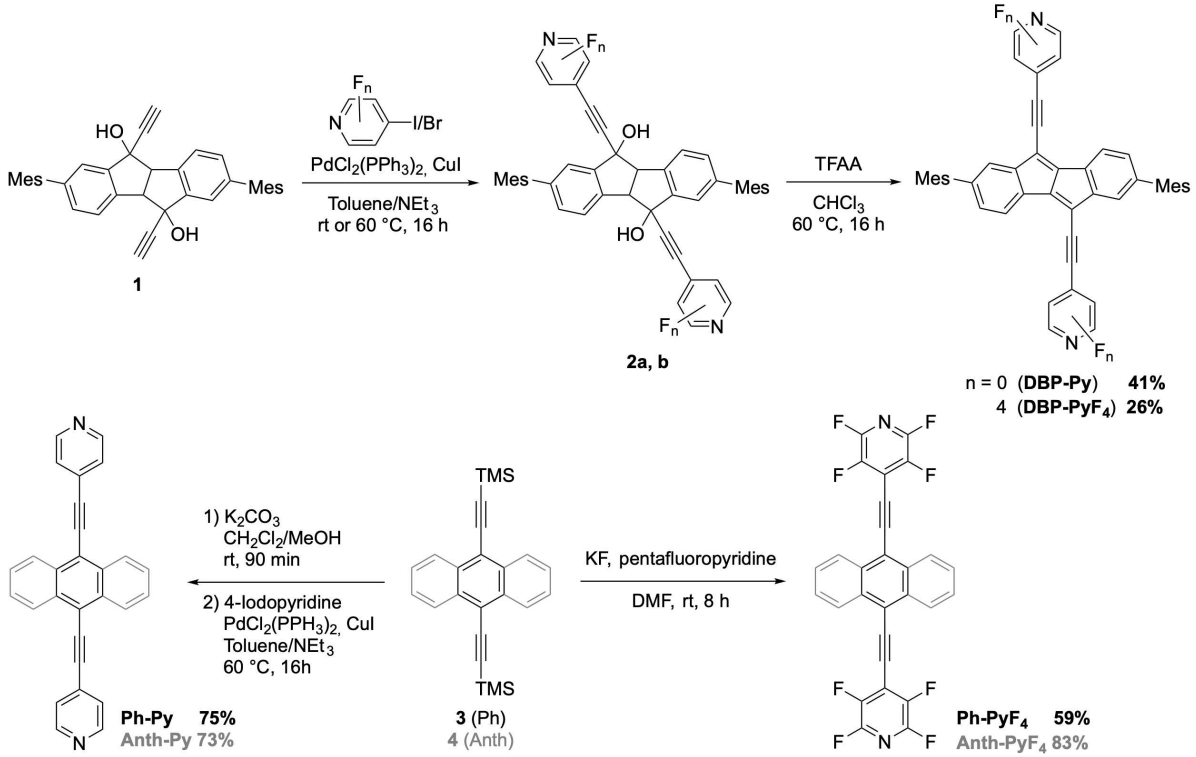

Scheme 1. Synthesis of investigated compounds.

idine to obtain **Ph-PyF$_4$** and **Anth-PyF$_4$** in good yields of 59% and 83%, respectively (for characterization as well as NICS-calculations, see SI).[23,24]

Break-Junction Measurements

The scanning tunneling microscope break-junction (STM-BJ) technique was used to measure the single-molecule conductance of each compound using typical methodology under ambient conditions and in the absence of solvent (full details are given in the Supporting Information, Section 8). Starting with **Ph-Py**, we found the conductance histogram peak position (i.e. the average junction conductance) was strongly correlated with the ratio of molecular junctions to empty junctions during any particular period. Previously, we have shown this phenomenon likely arises due to the presence of multiple molecules in or around the junction.[25] A detailed discussion of this behaviour for **Ph-Py** is given in the Supporting Information, Section 8.4. Based on this analysis, we concluded that the most appropriate method to compare the conductances of all compounds in this study as fairly as possible was to compare the signal recorded during periods of low plateau percentages, when the percentage is less than 50%. Furthermore, as it is possible that multiple molecular junctions can still form under such conditions, we separated plateau traces that contain a clear jump down to the noise and back again, which we previously termed "broken-plateaus" to distinguish them from continuous plateaus. Broken plateau traces have the highest likelihood to be due to pure single-molecule junctions due to the low probability multi-molecule junctions break and reattach simultaneously.

Figure 2a shows the 1D conductance (G) histograms built from the extracted broken-plateau traces recorded for **Ph-Py**, **Anth-Py** and **DBP-Py** during low-percentage periods (for the specific number of junctions recorded, see Table S3). Figure 2b displays the corresponding 2D G-z histograms (where G is the measured conductance in Siemens and G_0 is the quantum of conductance through a single channel ($G_0 = 7.75\times10^{-5}$ S) and z is the distance). The maxima of Gaussian fits to each 1D histogram are plotted in Figure 2c and tabulated in Table 1. It is evident that the average conductance increases following the general trend $G_{\text{Ph-Py}} < G_{\text{Anth-Py}} < G_{\text{DBP-Py}}$ (black squares). For comparison, we also show the conductance data of the previously reported thioanisole series (red circles, for structures see Figure S1) which we have reprocessed to extract the broken-plateau traces from low percentage periods to match the data processing of the pyridyls. Despite their shorter molecular lengths, for any given centre group the pyridyl compounds conduct slightly worse than the thioanisoles, which is in line with other studies comparing pyridyl and thioether anchor groups.[7,26] It is noteworthy that the relative conductance increase of **DBP-Py** over the phenyl and anthracene analogues is slightly higher than in the thioanisole series, which is suggestive of a slightly better energetic alignment between the closest frontier molecular orbital of **DBP-Py** and the gold Fermi level.

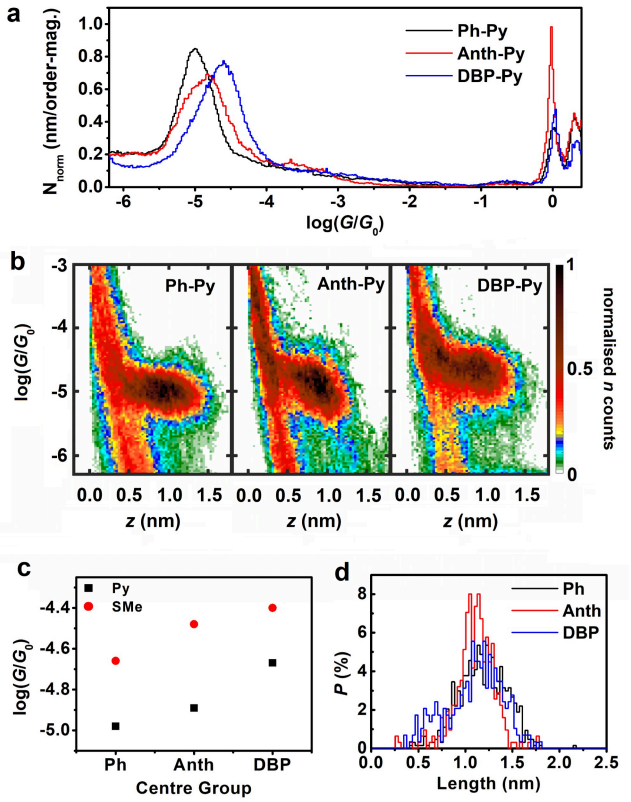

Figure 2. a) 1D conductance histograms built from broken-plateau traces for **Ph-Py**, **Anth-Py** and **DBP-Py**. b) Corresponding 2D histograms. c) 1D histogram peak positions plotted against central group for pyridyl and thioanisole anchor groups. d) Plateau-length histograms for pyridyl compounds showing the distribution in plateau lengths measured from just after the Au–Au junction breaks.

Table 1. Single molecule conductance and length data from STM-BJ experiments plus optical band gap.

Molecule	Measured conductance ($\log(G/G_0)$ [a]	Molecular X–X[b] distance (nm)	Measured most-frequent and maximal[c] distance + 0.5 nm	E_g (UV–vis) (eV) [d]
Ph-Py	−4.98 (0.52)	1.65	1.68 (2.14)	3.55
Anth-Py	−4.89 (0.74)	1.65	1.60 (1.90)	2.57
DBP-Py	−4.67 (0.69)	1.69	1.64 (2.14)	1.83
Ph-SMe	−4.66 (0.64)	2.01	1.78 (–)[e]	3.25
Anth-SMe	−4.48 (0.88)	2.02	1.63 (2.11)	2.48
DBP-SMe	−4.40 (0.91)	2.04	1.77 (2.17)	1.73

[a] Values in parentheses are the full-width at half-maxima. [b] X is either N (Py) or S (SMe). [c] Values at which the fitted peak falls to 80% of its maximum height. [d] Optical band gap from the onsets of the longest wavelength absorption band. [e] Too little data for accurate measurement.

Figure 2d shows the plateau length distributions as measured for the pyridyl derivatives with no correction applied for the electrode relaxation (so-called jump-out-of-contact, JOOC, which is usually 0.5 nm on average). The corrected most-frequent and maximal junction stretching distances are given in Table 1 along with the calculated molecular lengths (see section 8.2 in the SI for details on how we measure the plateau lengths). The optimised geometry of **Ph-Py** (calculated at the PBEh-3c level) as well as **Anth-Py** yields an N–N-distance = 1.65 nm, and an Au–Au distance = 2.05 nm (calculated by adding twice the radius of a gold atom plus twice the radius of a nitrogen atom). We see that the maximum observed plateau lengths correspond well to the Au–Au distance, which shows the molecules can be fully-stretched within a junction.

Generally, within each anchor group family, junctions with anthracene tend to be the shortest. In the case of the thioanisoles, we previously suggested this is due a weaker Au–S bond as a result of greater overall conjugation which reduces the donating ability of the S lone pairs towards gold. Further evidence of this conjugation-related effect was seen for a series of fluorene compounds, in which various anchor groups were connected either in either *para* or *meta* fashion. *Para*-coupling gives rise to greater overall conjugation and, therefore, slightly longer plateaus compared to *meta*. These results show that conjugation slightly undermines mechanical stability.

Conductance Versus Voltage Behaviour

To assess the Fermi level-frontier energy level alignment in junctions of **DBP-Py**, we carried out conductance versus voltage (*G-V*) measurements for each compound using a wide voltage range of ±1.5 V. A full description of the process is given in Section 8.3 in the SI. For this procedure, both continuous and broken-plateaus were considered. We stress that such large voltages are uncommon for molecular junctions, especially with dative attachments, where junctions typically become unstable and break down. We observed, however, that some junctions survived long enough for one or two voltage ramps to be completed. We therefore developed a selection procedure to extract only the *G-V* curves in which the junction survives the full duration of the ramp (i.e. from +1.5 V to −1.5 V). This methodology favours the most-strongly bound molecules, and the absolute measured conductance values tend to be higher than at fixed-bias. In order to compare the change in relative shape of the *G-V* traces, we normalised each individual *G-V* curve to the same low-bias value. This allows us to compare the relative change in conductance from low to high bias.

Figure 3a and b shows the averaged normalised $\log(G/G_0)$-*V* traces for Py and SMe anchor groups respectively. Clearly, the conductance increases with voltage for all compounds, a consequence of the Fermi level siting within the HOMO–LUMO gap. **Anth-SMe** and **DBP-SMe** were previously measured over a similar voltage range, but **Ph-SMe** was only measured between ±1.0 V,[19] and thus we repeated the measurement to extend the bias window to ±1.5 V. Generally, the increase in $\log(G/G_0)_{norm}$ is small for the phenyl derivatives, increasing by $\Delta\log(G/G_0)_{norm} \approx 0.25$ between 0 V and ±1.5 V for both anchor groups. This is due to their wide HOMO–LUMO gaps (see Table 1), where the Fermi level sits far from the closest molecular resonance (ε_0). The anthracene derivatives display a greater

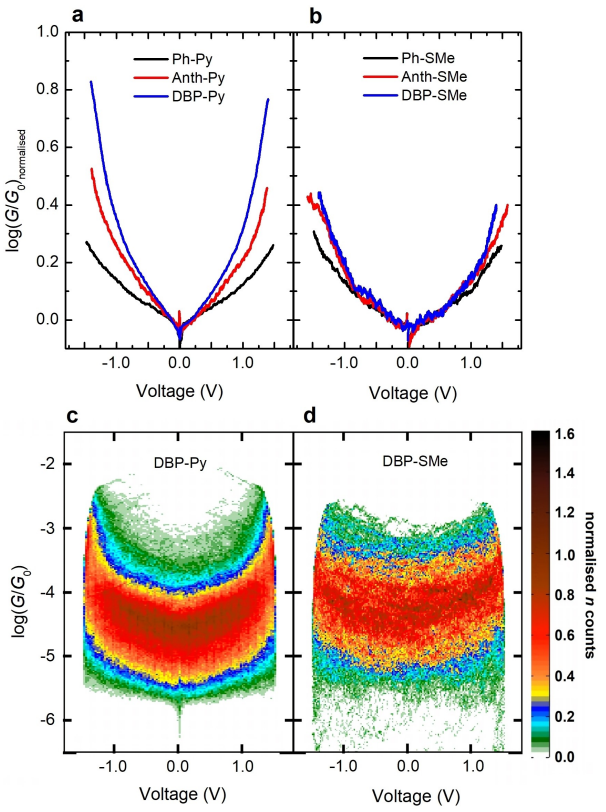

Figure 3. a) Normalised conductance *versus* voltage (log(G/G_0)-V) curves for pyridyl and b) for thioanisole compounds measured between ±1.5 V. c) and d) Non-normalised log(G/G_0)-V 2D histograms for **DBP-Py** and **DBP-SMe**, respectively. This allows the reader to see the measured conductance at a given bias voltage.

increase where $\Delta\log(G/G_0)_{norm} \approx 0.4$–$0.5$ for both, due to their lower HOMO–LUMO gaps. In the case of the DBP compounds, a clear and intriguing difference is seen between the two types of anchor group. Despite its lower HOMO–LUMO gap, the log(G/G_0)$_{norm}$-V curve of **DBP-SMe** is very similar to that of **Anth-SMe**, which implies that when inside a molecular junction, the difference between ε_0 and the Fermi level is similar in both junctions. The curve for **Anth-Py** is similar to that of **Anth-SMe**, but interestingly, now $\Delta\log(G/G_0)_{norm} \approx 0.8$ for **DBP-Py**. This means that at higher bias voltages, the conductance difference between **Anth-Py** and **DBP-Py** grows. The significance is that despite having similar HOMO–LUMO gaps, ε_0 lies significantly closer to the Fermi level for **DBP-Py**.

Figure 3c and d compares the (non-normalised) 2D log(G/G_0)-V histograms for **DBP-SMe** and **DBP-Py**. The rapid increase in conductance associated with approaching resonance is clearly seen for **DBP-Py** just beyond ±1.0 V, but is absent for **DBP-SMe**.[27,28] A consequence of the sharp increase in G is that **DBP-Py** becomes slightly more conductive than **DBP-SMe** at high bias. The bias voltage at which ε_0 comes into resonance with the Fermi level (V_{res}) can be estimated as

$$V_{res} = (E_F\text{-}\varepsilon_0)/\eta e$$

where η is the fraction of the bias voltage that drops between the molecule and the contacts and e is the elementary charge. If the left and right couplings of the molecule to the electrodes are equal, $\eta = 0.5$.[29] Assuming a HOMO–LUMO gap of 2 eV for both (based on our cyclic voltammetry (CV) study - see Table S2 in Section 7 of the SI for all oxidation and reduction potentials) V_{res} would be 2.0 V if E_F lies in the middle of the gap (*i.e.* E_F-ε_0 = 1 eV. This also assumes negligible change in the gap upon binding to gold). For **DBP-SMe**, V_{res} must be greater than 1.5 V (*i.e.* outside the measured voltage range) due to the lack of any sharp increase in G. This indeed implies that E_F indeed sits very close to the centre of the HOMO–LUMO gap. On the other hand, for **DBP-Py**, $V_{res} \approx 1.5$ V, which implies either the HOMO–LUMO gap of **DBP-Py** is smaller compared to **DBP-SMe** in the junction, or E_F sits closer to one of the frontier levels. We do not see an obvious reason the gap should change so much, so we believe that the alignment is the main difference.

The CV–measured onsets of oxidation and reduction give an estimation of the absolute positions of the HOMO and LUMO levels before attachment to gold (Table S2 in Section 7 in the SI). The CV-derived LUMO positions of **DBP-SMe** and **DBP-Py** are both significantly lower than the corresponding anthracene compounds (−3.15 eV for **Anth-SMe/Py** and −3.46 eV and −3.61 eV for **DBP-SMe** and **DBP-Py** respectively). The HOMOs too become slightly more negative when anthracene is exchanged for DBP. Overall, the observed behaviour is consistent with LUMO-dominated transport in **DBP-Py** and fits with previous studies on pyridyl-anchored compounds.[21]

Transport Calculations

To corroborate these findings, we conducted transport calculations on **Ph-Py**, **Anth-Py** and **DBP-Py** using a combination of density functional theory (DFT) and Green's function techniques as described in Section 9 in the SI and by Pauly *et al.*[30] and Zotti *et al.*[31] Figure 4 (lower panel) shows the gap-corrected transmission curves for the three compounds placed between gold clusters in a top-binding position as depicted in the upper panel of the same figure. Transport calculations for the thioanisole series have been previously reported.[19] We find that transport takes place through the tail of the LUMO-derived resonance for each compound. This resonance progressively approaches the Fermi level from **Ph-Py** to **Anth-Py** to **DBP-Py**, which follows the order in gas-phase LUMO energies (see Table S2 for the experimentally-derived orbital energies and Table S5 for the DFT calculated values). The trend in the transmission at the Fermi level matches the experimental low-bias conductances well and the results provides an explanation for the much greater voltage-dependence of **DBP-Py** thanks to the better LUMO-Fermi level alignment. We note that the magnitude of the transmission at the Fermi level is also very close to the experimentally determined low-bias conductance. Interestingly, whilst the LUMO-derived resonance has a Lorenzian line shape, the HOMO-derived resonance of **DBP-Py** is a Fano resonance, which is indicative of a localised state.[32,33] The gas-phase HOMO is localised mainly on the central DBP unit

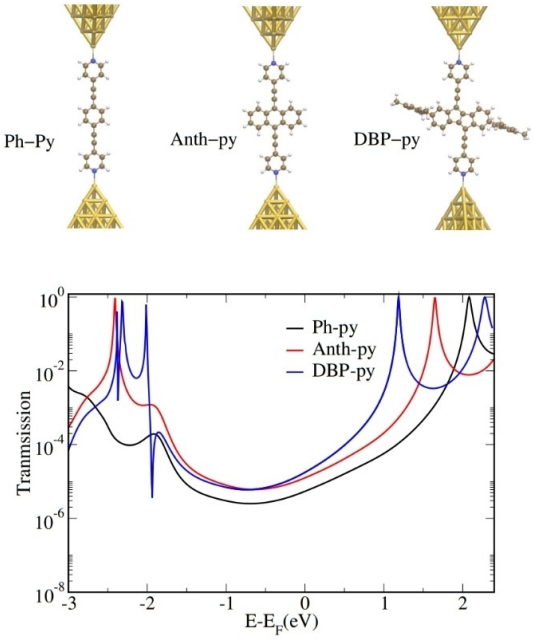

Figure 4. (Upper panel) Geometries of the junctions built for the transport calculations of **Ph-Py**, **Anth-Py** and **DBP-Py**. (Lower panel) Transmission as a function of energy for each compound.

whilst the LUMO is essentially delocalised over the entire molecule (see Figure S44 in the SI). The HOMO − 1 is also spread out over the entire molecule. The origin of the Fano resonance seems to be due to interference between the HOMO–1 and the long-axis of the localised HOMO, which sits perpendicular to the main transport axis. Instead, in the case of **Ph-Py** and **Anth-Py**, both HOMO and LUMO are fully extended, giving rise only to Lorenzian line shapes.

The influence of the energetic position of the molecular levels with respect to the Fermi level upon conductance has been well-studied. The alignment is well-known to be strongly influenced by the type of anchoring group.[10] On the other hand, numerous studies, both at the single-molecule level and on self-assembled monolayers, show that varying substituents attached to the backbone of molecular wires, and hence shifting the HOMO/LUMO energies, often has negligible effect on conductance.[25,34,35] This has been attributed to the Fermi level pinning effect which essentially restricts significant overlap between a frontier orbital and the Fermi level.[36] Here, conversely, the difference in conductance between phenyl and anthracene can be explained by the smaller gap of the latter, which brings *both* HOMO and LUMO closer to the Fermi level. In the case of DBP, as this group has more effect on the energetic position of the LUMO, we only see the effect of the lower gap upon transport when the anchor groups are pyridyl and, hence, LUMO transport.

Fluorinated Compounds

Finally, we discuss the results of the F4-pyridyl-terminated compounds. Our spectroscopic characterisation (Section 7, SI) shows that fluorination of the pyridyl groups results in slightly narrower HOMO–LUMO gaps and significantly lower-lying LUMO levels. This should result in an enhanced molecular conductance, particularly for **DBP-PyF4**. We attempted to measure the freshly-prepared samples, however, on each trial, we were unsuccessful in forming convincing molecular junctions (see section 8.5 in the SI for analysis and further details). This is despite a previous report on fluorinated dipyridyl compounds, where junctions did seem to form.[37] Here, we propose that, analogous to the way anthracene reduces the availability of the N lone pairs, the fluorine atoms deactivate them to the point that stable molecular junctions can no longer form. We computed the binding energy of the Py as well as the PyF4 series in the junction. The total binding energies for the Py compounds were similar and close to 1.4 eV (i.e. ~0.7 eV per side) whilst those of the PyF4 compounds were between 0.7–0.8 eV (~0.35 eV per side). This corresponds to an average reduction of about 50% in the binding strength of the fluorinated compared to the pristine compounds, supporting the experimental observations. The shorter compounds investigated by Velizhanin *et al.* will have less overall conjugation than those here, which explains why they could still form molecular junctions.

We conclude that F_4-pyridyls are, therefore, generally not good as anchor groups when attached to relatively highly-conjugated backbones.

Comparison with other Aromatic and Antiaromatic Compounds

We finally compare our conductance results with compounds measured by other groups. Firstly, **Ph-Py** has been measured by several groups, and to facilitate the comparison, we first discuss the most-probable conductances for the histograms generated using all the plateau-containing traces for both low and high-percentage periods. A single Gaussian curve fit to the low percentage histogram peak (Fig. S39a) gives a conductance of $\log(G/G_0) = -4.91$. The high percentage peak, on the other hand, does not fit well to a single Gaussian and the (approximate) centre of the peak is $\log(G/G_0) = -4.35$, which is almost four times higher. The low-conductance onset of both histograms is, however, very similar (ca. $\log(G/G_0) = -5.5$), which shows that the multi-molecule junctions formed during the high-percentage periods probably decay to a single-molecule junction just before complete rupture. Grunder *et al.* determined the conductance of **Ph-Py** using the mechanically-controllable break-junction technique with a reported value of 3.5×10^{-6} G_0 ($\log(G/G_0) = -5.46$) obtained as the position of the peak maximum of the linear-scale histogram.[38] This has been shown to correlate with the low-conductance onset of the peak in the log-scale histogram which, in our case, is in very good agreement.[39] Manrique *et al.* also measured the same compound, reporting a conductance of ($\log(G/G_0) = -4.5$, i.e. at the maximum of the log-histogram) with 100% junction-formation probability. This is similar to the position of the peak in our

high-percentage data, which suggests this measurement was dominated by multi-molecule junctions.[4]

The conductance of **DBP-Py** is about a factor two lower than **DBP-SMe**, despite its ε_0 lying closer to the Fermi level, and is essentially the same as **Ph-SMe**, despite this compound having a much wider HOMO–LUMO gap. This demonstrates the influence of the electronic coupling (normally represented as Γ) which is clearly poorer for pyridine versus thioanisole. A simple explanation of this is that the nitrogen-based lone pair in pyridine are orthogonal to the aromatic π-system and thus act more as mechanical linkers. Gantenbein at al. measured several pyridyl-endcapped biphenylenes, which are mildly antiaromtic. The 1,4 derivative (labelled compound 1 in their study) has a similar N–N distance as **DBP-Py** and a comparable conductance of $\log(G/G_0) = -4.6$, although in this study the plateau percentages were not reported. The conductance of a derivative of norcorrole attached with thiols (NiNc-SAc) was measured by Fujii et al, who found a value of $\log(G/G_0) = -3.4$, significantly higher than **DBP-Py**. This increase can mainly be explained by the thiol anchors, which are known to produce junctions with low contact resistance (i.e. they have large Γ). This is further borne out by **Ph-SAc**, which also forms gold-thiolate bonds, and has a $\log(G/G_0)$ peak at -3.7,[39] making it about one order of magnitude more conductive than **DBP-Py** at low bias.

The main point of this study was not to produce the most highly-conducting molecular junctions, rather to demonstrate that antiaromatic units can boost single-molecule conductance when paired with appropriate anchor groups. Our results show that it is unlikely that distortions to the π-system as a result of binding to the electrodes significantly affect the conductance as proposed.[40] This highlights the difficulty in drawing robust comparisons with charge transfer studies and single-molecule conductance experiments.[41] Looking forward, other robust LUMO-aligning anchor groups need to be explored that can produce junctions with much lower contact resistance than pyridyls. When paired with antiaromatic groups like DBP, we expect such compounds will produce junctions of higher conductance than their aromatic counterparts.

Conclusions

We have studied the single-molecule conductance of a family of pyridyl-terminated compounds containing a central phenyl, anthracene or dibenzopentalene (DBP) group. The phenyl and anthracene derivatives are fully aromatic compounds, whereas the DBP contains a central 8 π-electron antiaromatic subunit. Antiaromaticity leads to a low-lying LUMO level in the DBP compound resulting in the highest conductance and the greatest conductance-voltage response. The behaviour is more pronounced than in an analogous series using thioanisole anchor groups which is due to the way the anchor group affects the alignment of the molecular levels with respect to the Fermi level. These results show that the enhancement of molecular conductance due to antiaromaticity is anchor group-dependent, and is controlled by the relative positions of the frontier orbitals.

Supporting Information

Detailed description of materials and methods, synthetic procedures, chemical characterization, break junction methodology and details of the theoretical calculations are available in the Supporting Information file. The authors have cited additional references within the Supporting Information.[42–68]

Notes

The raw data that support the findings of this study, including individual traces (*G-z* and *I–V*) for the STM experiments, are freely available after acceptance of the manuscript at Zenodo under the following DOI: 10.5281/zenodo.10600543.

Acknowledgements

EL thanks the Comunidad de Madrid Atracción de Talento grant 2019-T1/IND-16384 and from the Spanish MCIN (MCIN/AEI/10.13039/501100011033) PID2021-127964NB-C21 and CNS2023-145464. IMDEA Nanociencia acknowledges support from the 'Severo Ochoa' Programme for Centres of Excellence in R&D (CEX2020-001039-S). TG thanks NanomagCOST-CM (S2018/NMT-4321) and DECOSMOL (EIGConcertJapan). This project was funded by the German Research Foundation (DFG) under Project ID 441236036 and through grant no INST 40/575-1 FUGG (JUSTUS 2 cluster). We acknowledge financial support through the state of Baden-Württemberg through bwHPC. LAZ thanks the Spanish MCIN/AEI/10.13039/ 501100011033 for the grant PID2021-125604NB-I00 and the "María de Maeztu" Programme for Units of Excellence in R&D (CEX2023-001316-M). Open Access funding enabled and organized by Projekt DEAL.

Conflict of Interests

The authors declare no conflict of interest.

Data Availability Statement

The data that support the findings of this study are openly available in Zenodo at https://doi.org/10.5281/zenodo.10600543, reference number 10600543.

Keywords: break junction · single-molecule conductance · antiaromaticity · dibenzopentalene · pyridyl anchor groups

[1] C. J. Lambert, *Chem. Soc. Rev.* **2015**, *44*, 875–888.
[2] X. Li, Z. Tan, X. Huang, J. Bai, J. Liu, W. Hong, *J. Mater. Chem. C* **2019**, *7*, 12790–12808.
[3] K. Yoshizawa, *Acc. Chem. Res.* **2012**, *45*, 1612–1621.
[4] D. Z. Manrique, C. Huang, M. Baghernejad, X. Zhao, O. A. Al-Owaedi, H. Sadeghi, V. Kaliginedi, W. Hong, M. Gulcur, T. Wandlowski, M. R. Bryce, C. J. Lambert, *Nat. Commun.* **2015**, *6*, 6389.
[5] L. A. Zotti, E. Leary, *Phys. Chem. Chem. Phys.* **2020**, *22*, 5638–5646.

[6] C. Tang, L. Huang, S. Sangtarash, M. Noori, H. Sadeghi, H. Xia, W. Hong, *J. Am. Chem. Soc.* **2021**, *143*, 9385–9392.
[7] A. Alanazy, E. Leary, T. Kobatake, S. Sangtarash, M. T. González, H.-W. Jiang, G. R. Bollinger, N. Agräit, H. Sadeghi, I. Grace, S. J. Higgins, H. L. Anderson, R. J. Nichols, C. J. Lambert, *Nanoscale* **2019**, *11*, 13720–13724.
[8] E. Leary, A. La Rosa, M. T. González, G. Rubio-Bollinger, N. Agraït, N. Martín, *Chem. Soc. Rev.* **2015**, *44*, 920–942.
[9] R. Stadler, K. W. Jacobsen, *Phys. Rev. B* **2006**, *74*.
[10] L. A. Zotti, T. Kirchner, J.-C. Cuevas, F. Pauly, T. Huhn, E. Scheer, A. Erbe, *Small* **2010**, *6*, 1529–1535.
[11] W. Chen, H. Li, J. R. Widawsky, C. Appayee, L. Venkataraman, R. Breslow, *J. Am. Chem. Soc.* **2014**, *136*, 918–920.
[12] M. Gantenbein, L. Wang, A. A. Al-jobory, A. K. Ismael, C. J. Lambert, W. Hong, M. R. Bryce, *Sci. Rep.* **2017**, *7*, 1794.
[13] A. Borges, G. C. Solomon, *J. Phys. Chem. C* **2017**, *121*, 8272–8279.
[14] Y. Yang, M. Gantenbein, A. Alqorashi, J. Wei, S. Sangtarash, D. Hu, H. Sadeghi, R. Zhang, J. Pi, L. Chen, X. Huang, R. Li, J. Liu, J. Shi, W. Hong, C. J. Lambert, M. R. Bryce, *J. Phys. Chem. C* **2018**, *122*, 14965–14970.
[15] D. Miguel, L. Álvarez de Cienfuegos, A. Martín-Lasanta, S. P. Morcillo, L. A. Zotti, E. Leary, M. Bürkle, Y. Asai, R. Jurado, D. J. Cárdenas, G. Rubio-Bollinger, N. Agraït, J. M. Cuerva, M. T. González, *J. Am. Chem. Soc.* **2015**, *137*, 13818–13826.
[16] S. Fujii, S. Marqués-González, J.-Y. Shin, H. Shinokubo, T. Masuda, T. Nishino, N. P. Arasu, H. Vázquez, M. Kiguchi, *Nat. Commun.* **2017**, *8*, 1–8.
[17] C. J. Kingsbury, M. O. Senge, *Coord. Chem. Rev.* **2021**, *431*, 213760.
[18] M. Gantenbein, X. Li, S. Sangtarash, J. Bai, G. Olsen, A. Alqorashi, W. Hong, C. J. Lambert, M. R. Bryce, *Nanoscale* **2019**, *11*, 20659–20666.
[19] M. Schmidt, D. Wassy, M. Hermann, M. T. González, N. Agräit, L. A. Zotti, B. Esser, E. Leary, *Chem. Commun.* **2021**, *57*, 745–748.
[20] D. C. Grenz, M. Schmidt, D. Kratzert, B. Esser, *J. Org. Chem.* **2018**, *83*, 656–663.
[21] J. R. Widawsky, P. Darancet, J. B. Neaton, L. Venkataraman, *Nano Lett.* **2012**, *12*, 354–358.
[22] I. M. Grace, G. Olsen, J. Hurtado-Gallego, L. Rincón-García, G. Rubio-Bollinger, M. R. Bryce, N. Agraït, C. J. Lambert, *Nanoscale* **2020**, *12*, 14682–14688.
[23] I. V. Alabugin, S. V. Kovalenko, *J. Am. Chem. Soc.* **2002**, *124*, 9052–9053.
[24] T. A. Zeidan, S. V. Kovalenko, M. Manoharan, R. J. Clark, I. Ghiviriga, I. V. Alabugin, *J. Am. Chem. Soc.* **2005**, *127*, 4270–4285.
[25] M. T. González, X. Zhao, D. Z. Manrique, D. Miguel, E. Leary, M. Gulcur, A. S. Batsanov, G. Rubio-Bollinger, C. J. Lambert, M. R. Bryce, N. Agraït, *J. Phys. Chem. C* **2014**, *118*, 21655–21662.
[26] S. Wu, M. T. Gonzalez, R. Huber, S. Grunder, M. Mayor, C. Schoenenberger, M. Calame, *Nat. Nanotechnol.* **2008**, *3*, 569–574.
[27] E. Leary, B. Limburg, A. Alanazy, S. Sangtarash, I. Grace, K. Swada, L. J. Esdaile, M. Noori, M. T. González, G. Rubio-Bollinger, H. Sadeghi, A. Hodgson, N. Agraıt, S. J. Higgins, C. J. Lambert, H. L. Anderson, R. J. Nichols, *J. Am. Chem. Soc.* **2018**, *140*, 12877–12883.
[28] J.-R. Deng, M. T. González, H. Zhu, H. L. Anderson, E. Leary, *J. Am. Chem. Soc.* **2024**, *146*, 3651–3659.
[29] F. Zahid, M. Paulsson, S. Datta, in *Advanced Semiconductor and Organic Nano-Techniques*, Academic Press, San Diego, **2003**, pp. 1–41.
[30] F. Pauly, J. K. Viljas, U. Huniar, M. Häfner, S. Wohlthat, M. Bürkle, J. C. Cuevas, G. Schön, *New J. Phys.* **2008**, *10*, 125019.
[31] L. A. Zotti, M. Bürkle, F. Pauly, W. Lee, K. Kim, W. Jeong, Y. Asai, P. Reddy, J. C. Cuevas, *New J. Phys.* **2014**, *16*, 015004.
[32] A. K. Ismael, I. Grace, C. J. Lambert, *Phys. Chem. Chem. Phys.* **2017**, *19*, 6416–6421.
[33] Y. Zheng, P. Duan, Y. Zhou, C. Li, D. Zhou, Y. Wang, L.-C. Chen, Z. Zhu, X. Li, J. Bai, K. Qu, T. Gao, J. Shi, J. Liu, Q.-C. Zhang, Z.-N. Chen, W. Hong, *Angew. Chem. Int. Ed.* **2022**, *61*, e202210097.
[34] Z. Xie, I. Bâldea, C. D. Frisbie, *J. Am. Chem. Soc.* **2019**, *141*, 3670–3681.
[35] Z. Xie, V. Diez Cabanes, Q. Van Nguyen, S. Rodriguez-Gonzalez, L. Norel, O. Galangau, S. Rigaut, J. Cornil, C. D. Frisbie, *ACS Appl. Mater. Interfaces* **2021**, *13*, 56404–56412.
[36] C. Van Dyck, V. Geskin, J. Cornil, *Adv. Funct. Mater.* **2014**, *24*, 6154–6165.
[37] K. A. Velizhanin, T. A. Zeidan, I. V. Alabugin, S. Smirnov, *J. Phys. Chem. B* **2010**, *114*, 14189–14193.
[38] S. Grunder, R. Huber, S. Wu, C. Schönenberger, M. Calame, M. Mayor, *Eur. J. Org. Chem.* **2010**, *2010*, 833–845.
[39] R. Huber, M. T. Gonzalez, S. Wu, M. Langer, S. Grunder, V. Horhoiu, M. Mayor, M. R. Bryce, C. Wang, R. Jitchati, C. Schoenenberger, M. Calame, *J. Am. Chem. Soc.* **2008**, *130*, 1080–1084.
[40] A. Mahendran, P. Gopinath, R. Breslow, *Tetrahedron Lett.* **2015**, *56*, 4833–4835.
[41] R. Breslow, F. W. Foss, *J. Phys. Condens. Matter* **2008**, *20*, 374104.
[42] D. Bradley, G. Williams, M. Lawton, *J. Org. Chem.* **2010**, *75*, 8351.
[43] G. R. Fulmer, A. J. M. Miller, N. H. Sherden, H. E. Gottlieb, A. Nudelman, B. M. Stoltz, J. E. Bercaw, K. I. Goldberg, *Organometallics* **2010**, *29*, 2176–2179.
[44] R. K. Harris, E. D. Becker, S. M. Cabral de Menezes, R. Goodfellow, P. Granger, R. K. Harris, P. Granger, E. D. Becker, R. Goodfellow, S. M. Cabral de Menezes, R. Goodfellow, P. Granger, R. K. Harris, P. Granger, E. D. Becker, R. Goodfellow, *Magn. Reson. Chem.* **2002**, *40*, 489–505.
[45] J. Wilbuer, D. C. Grenz, G. Schnakenburg, B. Esser, *Org. Chem. Front.* **2017**, *4*, 658–663.
[46] S. Colella, M. Mazzeo, R. Grisorio, E. Fabiano, G. Melcarne, S. Carallo, M. D. Angione, L. Torsi, G. P. Suranna, F. Della Sala, P. Mastrorilli, G. Gigli, *Chem. Commun.* **2010**, *46*, 6273–6275.
[47] TURBOMOLE V7.5, a Development of University of Karlsruhe and Forschungszentrum Karlsruhe GmbH,1989-2007, TURBOMOLE GmbH, **2020**.
[48] M. J. Frisch, G. W. Trucks, H. B. Schlegel, G. E. Scuseria, M. A. Robb, J. R. Cheeseman, G. Scalmani, V. Barone, G. A. Petersson, H. Nakatsuji, X. Li, M. Caricato, A. V. Marenich, J. Bloino, B. G. Janesko, R. Gomperts, B. Mennucci, H. P. Hratchian, J. V. Ortiz, A. F. Izmaylov, J. L. Sonnenberg, Williams, F. Ding, F. Lipparini, F. Egidi, J. Goings, B. Peng, A. Petrone, T. Henderson, D. Ranasinghe, V. G. Zakrzewski, J. Gao, N. Rega, G. Zheng, W. Liang, M. Hada, M. Ehara, K. Toyota, R. Fukuda, J. Hasegawa, M. Ishida, T. Nakajima, Y. Honda, O. Kitao, H. Nakai, T. Vreven, K. Throssell, J. A. Montgomery Jr., J. E. Peralta, F. Ogliaro, M. J. Bearpark, J. J. Heyd, E. N. Brothers, K. N. Kudin, V. N. Staroverov, T. A. Keith, R. Kobayashi, J. Normand, K. Raghavachari, A. P. Rendell, J. C. Burant, S. S. Iyengar, J. Tomasi, M. Cossi, J. M. Millam, M. Klene, C. Adamo, R. Cammi, J. W. Ochterski, R. L. Martin, K. Morokuma, O. Farkas, J. B. Foresman, D. J. Fox, Gaussian 16 Rev. C.01, Gaussian, Inc., Wallingford CT, **2016**.
[49] K. Eichkorn, O. Treutler, H. Öhm, M. Häser, R. Ahlrichs, *Chem. Phys. Lett.* **1995**, *240*, 283–290.
[50] S. Grimme, J. Antony, S. Ehrlich, H. Krieg, *J. Chem. Phys.* **2010**, *132*, 154104.
[51] S. Grimme, S. Ehrlich, L. Goerigk, *J. Comput. Chem.* **2011**, *32*, 1456–1465.
[52] A. D. Becke, E. R. Johnson, *J. Chem. Phys.* **2005**, *123*, 154101.
[53] E. R. Johnson, A. D. Becke, *J. Chem. Phys.* **2006**, *124*, 174104.
[54] S. Grimme, J. G. Brandenburg, C. Bannwarth, A. Hansen, *J. Chem. Phys.* **2015**, *143*.
[55] M. Bühl, C. van Wüllen, *Chem. Phys. Lett.* **1995**, *247*, 63–68.
[56] P. von R Schleyer, C. Maerker, A. Dransfeld, H. Jiao, N. J. R. van Eikema Hommes, *J. Am. Chem. Soc.* **1996**, *118*, 6317–6318.
[57] M. Häser, R. Ahlrichs, H. P. Baron, P. Weis, H. Horn, *Theor. Chim. Acta* **1992**, *83*, 455–470.
[58] G. A. Petersson, A. Bennett, T. G. Tensfeldt, M. A. Al-Laham, W. A. Shirley, J. Mantzaris, *J. Chem. Phys.* **1988**, *89*, 2193–2218.
[59] R. Gershoni-Poranne, A. Stanger, *Chem. Eur. J.* **2014**, *20*, 5673–5688.
[60] A. Stanger, *J. Org. Chem.* **2010**, *75*, 2281–2288.
[61] A. Rahalkar, A. Stanger, "Aroma," can be found under http://schulich.technion.ac.il/Amnon Stanger.htm, **2014**.
[62] A. Stanger, *J. Org. Chem.* **2006**, *71*, 883–893.
[63] B. W. D'Andrade, S. Datta, S. R. Forrest, P. Djurovich, E. Polikarpov, M. E. Thompson, *Org. Electron.* **2005**, *6*, 11–20.
[64] R. Ahlrichs, M. Bär, M. Häser, H. Horn, C. Kölmel, *Chem. Phys. Lett.* **1989**, *162*, 165–169.
[65] A. Schäfer, H. Horn, R. Ahlrichs, *J. Chem. Phys.* **1992**, *97*, 2571–2577.
[66] J. P. Perdew, *Phys. Rev. B* **1986**, *34*, 7406–7406.
[67] S. Y. Quek, L. Venkataraman, H. J. Choi, S. G. Louie, M. S. Hybertsen, J. B. Neaton, *Nano Lett.* **2007**, *7*, 3477–3482.
[68] M. E. Björketun, Z. Zeng, R. Ahmed, V. Tripkovic, K. S. Thygesen, J. Rossmeisl, *Chem. Phys. Lett.* **2013**, *555*, 145–148.

Manuscript received: March 6, 2024
Accepted manuscript online: May 16, 2024
Version of record online: ■■, ■■

RESEARCH ARTICLE

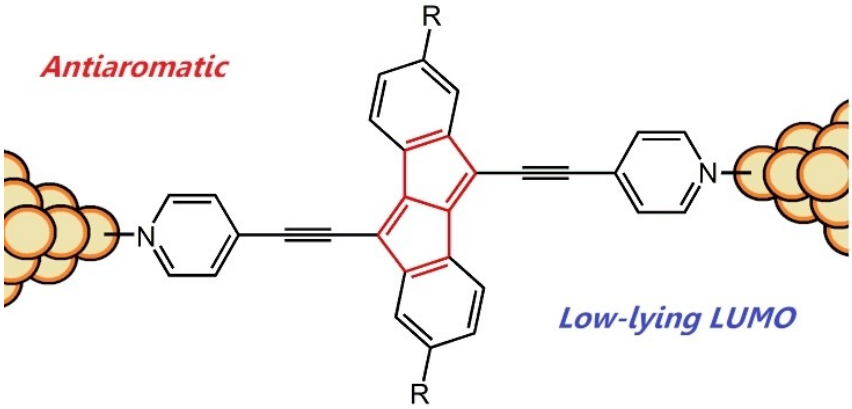

M. Schmidt, L. Abellán Vicente, Dr. M. T. González, Dr. L. A. Zotti, Prof. Dr. B. Esser*, Dr. E. Leary**

Dibenzopentalene paired with pyridyl anchor groups is shown to conduct better than aromatic analogues containing phenyl or anthracene inside single-molecule junctions. Compared to thioanisole anchors, pyridyls provide better molecular orbital level-Fermi level alignment. The result is a significant conductance-voltage response especially for a sub-2 nm long molecule. The conductance increases nearly ten-fold over a 1.5 V range.